Distributed Source-coding, Channel-coding and Modulation for Cooperative Communications

Soon Xin Ng, Kai Zhu and Lajos Hanzo
School of Electronics and Computer Science, University of Southampton, SO17 1BJ, United Kingdom.
Tel: +44-23-8059 3125, Fax: +44-23-8059 4508
Email: {sxn,kz1e08,lh}@ecs.soton.ac.uk, http://www-mobile.ecs.soton.ac.uk

***Abstract*— In this contribution, we propose a novel Distributed Source-coding, Channel-coding and Modulation (DSCM) scheme for cooperative communications. The proposed DSCM scheme is designed for ensuring the decoding convergence of its constituent component codes, namely, the Variable Length Code (VLC) and two Coded Modulation (CM) schemes. The source node encodes the source symbols with the aid of a serially-concatenated VLC and a Turbo Trellis Coded Modulation (TTCM) scheme. The TTCM-VLC encoded symbols are transmitted to both a relay node and to the destination node during the first transmission period. The relay node employs a powerful iterative TTCM-VLC decoder for estimating the VLC-encoded bit sequence. This decoded bit sequence is then re-encoded with the aid of a simple Trellis Coded Modulation (TCM) scheme before it is transmitted to the destination node. At the destination node, a novel four-component iterative decoding arrangement is invoked for recovering the original source symbols. It is shown that the DSCM scheme significantly outperforms the TTCM-VLC benchmarker scheme dispensing with relaying. The proposed power- and bandwidth-efficient DSCM scheme is an ideal candidate for next-generation mobile multimedia systems.**

***Index Terms*— Cooperative Diversity, Turbo Trellis Coded Modulation, Distributed Coding, Variable Length Codes.**

I. Introduction

Turbo Trellis Coded Modulation (TTCM) [1] is a joint coding and modulation scheme that has a structure similar to that of the family of binary turbo codes [2], [3], where two identical parallel-concatenated Trellis Coded Modulation (TCM) [4] schemes are employed as component codes. The design of a TTCM scheme was outlined in [1], which was based on the search for the best component TCM codes using the so-called 'punctured' minimal distance criterion for approaching the capacity of the Additive White Gaussian Noise (AWGN) channel. Recently, various TTCM schemes were designed in [5] with the aid of Extrinsic Information Transfer (EXIT) charts [6], [7] and union bounds for approaching the capacity of the Rayleigh fading channel.

Variable Length Codes (VLCs) constitute a family of low-complexity lossless source compression schemes. In order to exploit the residual redundancy of VLCs, numerous trellis-based VLC decoding techniques have been proposed, such as the joint source/channel coding scheme of [8], where the VLC decoder uses the bit-based trellis structure of [9]. Explicitly, in [8] a reversible VLC [10] was invoked as the outer code and a convolutional code was utilised as the inner code. In order to improve both the bandwidth and power efficiency of the joint source/channel coding scheme contrived in [8], various near-capacity jointly optimised source-coding, channel-coding and modulation schemes were proposed in [11]. It was shown in [11] that the TTCM assisted VLC (TTCM-VLC) scheme was the best performer among a range of Coded Modulation (CM) assisted VLC schemes, when communicating over Single-Input Single-Output (SISO) Rayleigh fading channels. However, the multimedia-rich wireless communication systems of future generations are required to provide reliable transmissions at high data rates.

The financial support of the EPSRC UK and that of the European Union under the auspices of the Optimix project is gratefully acknowledged.

Space time coding schemes [12], which employ multiple transmitters and receivers, are among the most efficient techniques designed for providing high data rates and substantial diversity gains by exploiting the high capacity potential of Multiple-Input Multiple-Output (MIMO) channels [13], [14]. However, it is difficult to eliminate the correlation of the signals when using multiple antennas at the mobile unit due to its limited size. In order to circumvent this problem, cooperative diversity schemes were proposed in [15]–[17]. More specifically, each mobile unit collaborates with either a single or a few partners for the sake of reliably transmitting its own information and of its partners jointly, which emulates a virtual MIMO scheme. The two most popular collaborative protocols used between the source, relay and destination nodes are the Decode-And-Forward (DAF) as well as the Amplify-And-Forward (AAF) schemes. However, a strong channel code is required for mitigating the potential error propagation in the DAF scheme or to mitigate the noise enhancement in the AAF scheme.

Distributed turbo codes [18] have been proposed for cooperative communications, although typically under the simplifying assumption of having a perfect communication link between the source and the relay nodes. It was found in [19] that three-component turbo codes are more beneficial in cooperative communications, when the realistic condition of having an imperfect source-relay communication link is taken into consideration. The power and bandwidth efficient Distributed TTCM (DTTCM) scheme proposed in [19] employs a conventional two-component TTCM at the source node and another TCM component code at the relay node in order to minimise the decoding errors at both the relay and the destination nodes. In this contribution, we further extend the concept of DTTCM proposed in [19] for assisting the TTCM-VLC scheme advocated in [11]. The Distributed Source-coding, Channel-coding and Modulation (DSCM) scheme advocated significantly outperforms the TTCM-VLC scheme due to the employment of a novel four-component iterative detection philosophy at the destination node.

The paper is organised as follows. The system model is described in Section II. The novel DSCM encoder and decoder are highlighted in Section III. The design and analysis of the proposed scheme is provided in Section IV and its performance is evaluated in Section V. Finally, our conclusions are offered in Section VI.

II. System Model

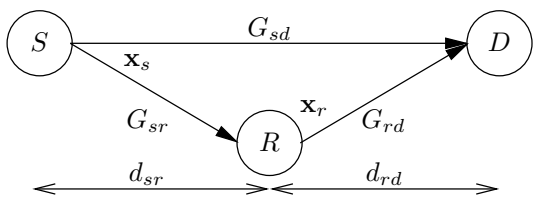

Fig. 1. Schematic of a two-hop relay-aided system, where d_{ab} is the geographical distance between node a and node b.

978-1-4244-3574-6/10/$25.00 ©2010 Crown

The schematic of a two-hop relay-aided system is shown in Fig. 1, where the source node (s) transmits a frame of coded symbols $\mathbf{x}_s$ to both the relay node (r) and to the destination node (d) during the first transmission period, while the relay node first decodes the information and then re-encodes it and finally transmits a frame of coded symbols $\mathbf{x}_r$ to the destination node during the second transmission period. The communication links seen in Fig. 1 are subject to both long-term free-space path loss as well as to short-term uncorrelated Rayleigh fading. The geometrical-gain [20] experienced by the source-to-relay link with respect to the source-to-destination link as a benefit of its reduced distance and path loss can be computed as:

$$G_{sr} = \left(\frac{d_{sd}}{d_{sr}}\right)^{\alpha} , \tag{1}$$

where d_{ab} denotes the geometrical distance between nodes a and b while α is the path loss exponent. We assume a free-space path loss model where the corresponding path loss exponent is given by $\alpha = 2$. The path loss exponent can be higher than 4 at suburban environment [21]. Similarly, the geometrical-gain at the relay-to-destination link with respect to the source-to-destination link can be formulated as:

$$G_{rd} = \left(\frac{d_{sd}}{d_{rd}}\right)^{2} . \tag{2}$$

Naturally, the geometrical-gain at the source-to-destination link with respect to itself is unity, i.e. we have $G_{sd} = 1$.

The kth signal received at the relay node during the first transmission period, where N_s symbols are transmitted from the source node, can be written as:

$$y_{r,k} = \sqrt{G_{sr}}\ h_{sr,k}\ x_{s,k} + n_{r,k} , \tag{3}$$

where $k \in \{1, \ldots, N_s\}$ and $h_{sr,k}$ is the Rayleigh fading coefficient between the source node and the relay node at instant k, while $n_{r,k}$ is the AWGN having a variance of $N_0/2$ per dimension. By contrast, the kth received symbol at the destination node during the first transmission period can be expressed as:

$$y_{d,k} = h_{sd,k}\ x_{s,k} + n_{d,k} , \tag{4}$$

where $h_{sd,k}$ is the Rayleigh fading coefficient between the source node and the destination node at instant k, while $n_{d,k}$ is the AWGN having a variance of $N_0/2$ per dimension. Similarly, the jth symbol received at the destination node during the second transmission period, where N_r symbols are transmitted from the relay node, is given by:

$$y_{d,j} = \sqrt{G_{rd}}\ h_{rd,j}\ x_{r,j} + n_{d,j} , \tag{5}$$

where $j \in \{1 + N_s, \ldots, N_r + N_s\}$ and $h_{rd,j}$ is the Rayleigh fading coefficient between the relay node and the destination node at instant j, while $n_{d,j}$ is the AWGN having a variance of $N_0/2$ per dimension.

If $x_{a,j}$ is the jth symbol transmitted from node a, the average received Signal to Noise power Ratio (SNR) at node b is given by:

$$\text{SNR}_r = \frac{\text{E}\{G_{ab}\}\text{E}\{|h_{ab,j}|^2\}\text{E}\{|x_{a,j}|^2\}}{N_0} = \frac{G_{ab}}{N_0} , \tag{6}$$

where $\text{E}\{|h_{ab,j}|^2\} = 1$ and $\text{E}\{|x_{a,j}|^2\} = 1$. For the ease of analysis, we define the ratio of the power transmitted from node a to the noise power encountered at the receiver of node b as:

$$\text{SNR}_t = \frac{\text{E}\{|x_{a,j}|^2\}}{N_0} = \frac{1}{N_0} . \tag{7}$$

Hence, we have:

$$\begin{aligned} \text{SNR}_r &= \text{SNR}_t\ G_{ab} , \\ \gamma_r &= \gamma_t + 10\log_{10}(G_{ab})\ [\text{dB}] , \end{aligned} \tag{8}$$

where $\gamma_r = 10\log_{10}(\text{SNR}_r)$ and $\gamma_t = 10\log_{10}(\text{SNR}_t)$. Hence, we can achieve a desired SNR_r by changing the transmit power or by selecting a relay at a different geographical location.

Similar to [11], we employ the reversible VLC[1] from [10], where the codewords are $C = \{00, 11, 010, 101, 0110\}$ associated with the source symbol sequence of $u = \{0, 1, 2, 3, 4\}$. The probabilities of occurrence for the symbols u are $P(u) = \{0.33, 0.30, 0.18, 0.10, 0.09\}$. The associated entropy is $L_s = 2.1391$ bits/symbol and the average codeword length is $L_{vlc} = 2.46$ bits/symbol, giving a VLC coding rate of $R_{vlc} = L_s/L_{vlc} = 0.8695$. Furthermore, a 16QAM-based TTCM encoder is used at the source node and a 16QAM-based TCM encoder is invoked at the relay node. Memory-three TCM codes having an octally represented generator polynomial of $[11\ \ 2\ \ 4\ \ 10]_8$ is used for both the TCM and TTCM encoder.

The overall throughput of this two-hop cooperative scheme can be computed as:

$$\eta = \frac{N_i}{N_s + N_r} \approx 1.3\ [\text{bps}] , \tag{9}$$

where N_i is the number of information bits transmitted within a duration of $(N_s + N_r)$ symbol periods. Again, N_s is the number of modulated symbols per frame emanating from the source node and N_r is the number of modulated symbols per frame transmitted from the relay node. We have $N_s = N_r$ in our case. We do not employ trellis termination for the TCM/TTCM encoder and we have $N_i = m\ R_{vlc}\ N_s \approx 2.6\ N_s$, where $m = 3$ for the 16QAM-based TCM and TTCM schemes. If an idealistic source compression (encoder) is considered, we have $L_{vlc} = L_s = 2.1391$ and $R^0_{vlc} = 1.0$. The DTTCM scheme of [19], which employs 8PSK modulation has a throughput of $\eta_{dttcm} = 1.33$ bps. Hence, when an idealistic source encoder is assumed the throughput of the DTTCM scheme in [19] will remain as $\eta_{dttcm} \times R^0_{vlc} = 1.33$ bps[2].

Without loss of generality, we assume that the relay node is located on a direct path between the source and destination nodes. Hence, we have:

$$d_{sd} = d_{sr} + d_{rd} . \tag{10}$$

Then, from Eqs. (1), (2) and (10), we have:

$$1 = \frac{1}{\sqrt{G_{sr}}} + \frac{1}{\sqrt{G_{rd}}} , \tag{11}$$

$$G_{rd} = \left(\frac{1}{1 - 1/\sqrt{G_{sr}}}\right)^2 . \tag{12}$$

We assume furthermore that the transmit power at the source node equals the transmit power at the relay node[3], i.e. the SNR_t at the source node ($\gamma_{t,sr}$) equals the SNR_t at the relay node ($\gamma_{t,rd}$), then:

$$\gamma_{t,rd} = \gamma_{t,sr} , \tag{13}$$

$$\gamma_{r,rd} - 10\log_{10}(G_{rd}) = \gamma_{r,sr} - 10\log_{10}(G_{sr}) , \tag{14}$$

$$\frac{G_{rd}}{G_{sr}} = 10^{\gamma_{d-r}/10} , \tag{15}$$

where $\gamma_{d-r} = \gamma_{r,rd} - \gamma_{r,sr}$ is the difference between the receiver's SNR at the destination during the second transmission period and the receiver's SNR at the relay during the first transmission period.

[1]Our design is applicable to any VLCs. However, the reversible VLC is good for iterative detection because it has a minimum free distance of 2 [22].

[2]If a Huffman code is use, we have $L_{vlc} = 2.19$ and $R_{vlc} \approx 0.98$ resulting in a throughput of $1.33 \times 0.98 \approx 1.3$ bps.

[3]It is also possible to design the system by fixing the relay location and then determine the appropriate transmit power levels for the source and relay nodes.

If $\gamma_{r,sr}$ is fixed at $\gamma_{r,sr} = \gamma_{r,sr\,\min}$ while $\gamma_{t,rd} = \gamma_{t,sr}$, then from Eqs. (12) and (15) we have:

$$G_{sr} \quad = \quad 10^{(\gamma_{r,sr\,\min} - \gamma_{t,sr})/10} \ , \tag{16}$$

and G_{rd} can be calculated based on Eq. (12) after G_{sr} is determined from Eq. (16). The average SNR_t per modulated symbol during the two transmission periods is given by:

$$\gamma_t \quad = \quad \frac{N_s\ \gamma_{t,sr} + N_r\ \gamma_{t,rd}}{N_s + N_r}\ [\text{dB}] \ . \tag{17}$$

Since we have $N_s = N_r$ and $\gamma_{t,sr} = \gamma_{t,rd}$, Eq. (17) can be simplified to $\gamma_t = \gamma_{t,sr} = \gamma_{t,rd}$.

III. DSCM Structure

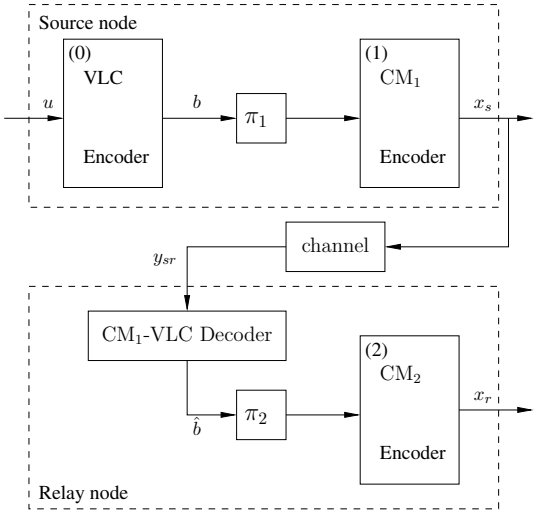

Fig. 2. The schematic of the DSCM encoder.

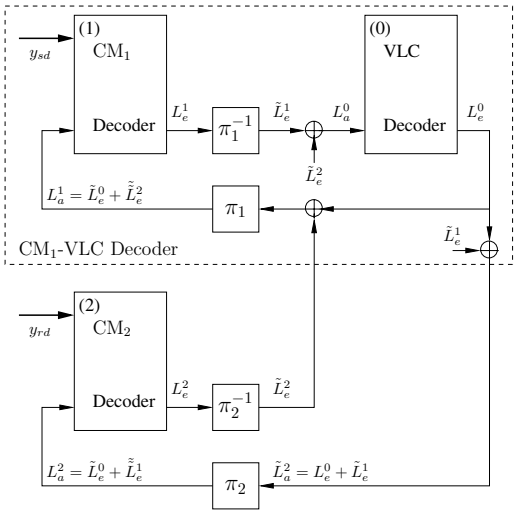

Fig. 3. The schematic of the DSCM decoder.

The general schematics of the DSCM encoder and decoder are shown in Fig. 2 and Fig. 3, respectively. More specifically, we have selected TTCM for the CM_1 block to assist the VLC scheme, since TTCM-VLC arrangement was found to be the best scheme among a range of other CM-VLC schemes [11]. At the relay node, we have chosen TCM for the CM_2 block. Note that we need a different bit interleaver π_2 at the relay, as compared to that at the source node, π_1, in order to achieve the full potential of the additional TCM component at the relay node. The CM_1-VLC (or TTCM-VLC) decoder of the relay node is a three-component decoder [11, Fig. 3], while the DSCM decoder is a four-component decoder incorporating both the three-component TTCM-VLC decoder (as shown at the top of Fig. 3) and an additional CM_2 (or TCM) decoder (as shown at the bottom of Fig. 3). As seen in Fig. 3, the DSCM decoder is specifically designed to ensure that each of the constituent decoder benefits from the extrinsic information of other constituent decoders through the *a priori* probability input, which is constituted by the interleaved (or deinterleaved) version of the *extrinsic* probability generated from the other constituent decoders.

IV. Design and Analysis

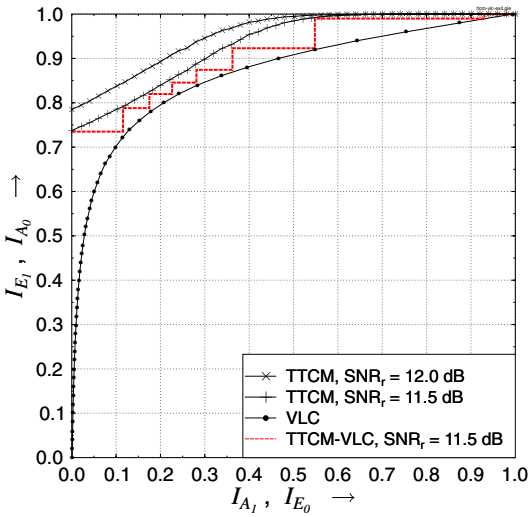

Fig. 4. The EXIT curves of the TTCM-VLC scheme for non-cooperative scenario. This corresponds also to the TTCM-VLC performance at the source-to-relay link where the SNR shown is the receiver SNR which is related to the transmit SNR and the geometrical-gain G_{sr}. The TTCM decoder employs 4 internal iterations.

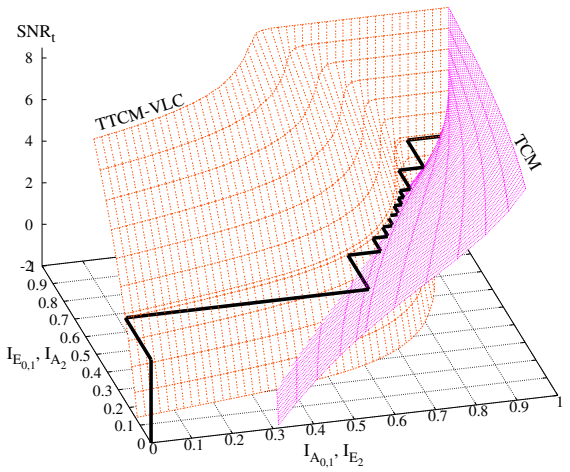

Fig. 5. The 3D EXIT chart of the TTCM-VLC and TCM decoders at the destination node employing a relay located at the mid-point between the source and destination node. The decoding trajectory of the DSCM decoder is computed at $\text{SNR}_t = 2$ dB assuming a perfect relay. The TTCM decoder employs 2 internal iterations and 4 outer iterations with the VLC decoder.

In order to minimise the decoding errors at the relay node, we first need to find the minimum required receive SNR at the relay. We can find this value either from simulation or from the EXIT chart of the TTCM-VLC decoder. The EXIT chart of the TTCM-VLC decoder recorded for the classic non-cooperative scenario is shown in Fig. 4, where the decoding trajectory is computed based on a frame length of 15 000 16QAM symbols. When there is no geometrical-gain, i.e. $G_{sd} = 1$, we have SNR_r=SNR_t. As we can see from Fig. 4 a receive

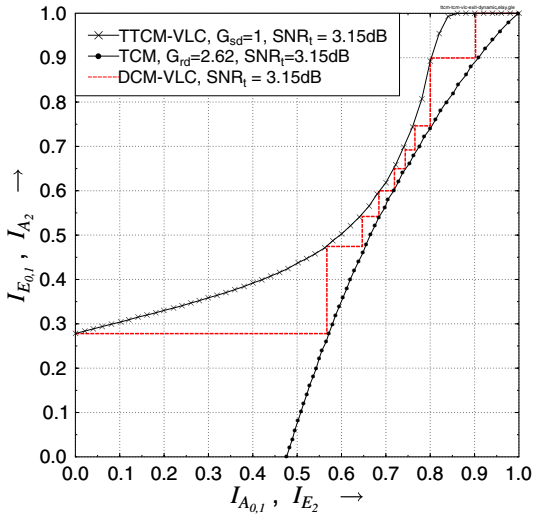

Fig. 6. The EXIT curves of the DSCM scheme at $\text{SNR}_t = 3.15$ dB. The TTCM decoder employs 2 internal iterations and 4 outer iterations with the VLC decoder. The relay is located at $d_{rd} = 0.6174\, d_{sd}$ ($d_{sr} = 0.3826\, d_{sd}$).

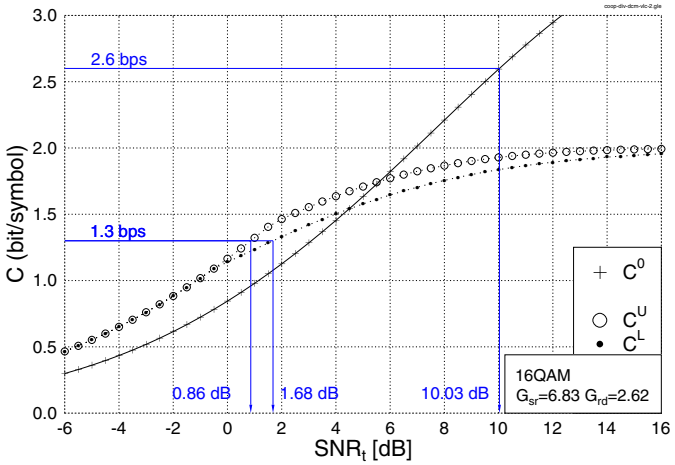

Fig. 7. DCMC capacity curves of the 16QAM-based cooperative and non-cooperative schemes. The 16QAM-based non-cooperative channel capacity C^0 is computed based on [23], while the upper bound C^{U} and lower bound C^{L} of the relay channel are computed based on Eqs. (18) and (19), respectively.

SNR of 11.5 dB is needed for attaining a decoding convergence after eight decoding iterations between the TTCM decoder and the VLC decoder. The BER versus SNR_t of the TTCM-VLC employing eight decoding iterations is shown in Fig. 8, which verifies the EXIT chart prediction portrayed in Fig. 4. When TTCM-VLC decoder is used at the relay node, the corresponding SNR_t can be computed based on Eq. (8) for a given G_{sr} value.

Fig. 5 shows the 3-Dimensional (3D) EXIT chart of the DSCM scheme, when the relay is located at the mid-point between the source and destination node, i.e. we have $G_{sr} = G_{rd} = 4$. The DSCM decoding trajectory is computed at $\text{SNR}_t = 2$ dB based on the idealised perfect relaying case, where there are no decoding errors at the relay. However, the BER performance of the DSCM scheme employing realistic relaying subject to error propagation, as shown in Fig. 8, requires $\text{SNR}_t = 5.5$ dB for achieving a high decoding convergence. This is due to the potential error propagation from the relay, which requires a minimum of $\text{SNR}_t = 11.5 - 10\log_{10}(G_{sr}) = 5.5$ dB for avoiding error propagation from the relay, when we have $G_{sr} = 4$.

The next step in our design is to choose an optimal relay based on its geographical location. By fixing the receive SNR at the relay node to 11.5 dB, we found that the DSCM can achieve a decoding convergence at $\text{SNR}_t = 3.15$ dB as shown in the EXIT curves in Fig. 6 when the relay is located at $d_{rd} = 0.6174\, d_{sd}$ ($d_{sr} = 0.3826\, d_{sd}$) which gives $G_{sr} = 6.83$ and $G_{rd} = 2.62$. We call the DSCM scheme employing a relay at the optimal location as DSCM-O.

V. Performance Evaluation

The Discrete-Input Continuous-Output Memoryless Channel (DCMC) [23] capacity, C^0, of a non-cooperative 16QAM-based scheme is shown in Fig. 7. The upper and lower bounds of the DCMC capacity of the two-hop half-duplex relay network can be computed based on [24], [25] as Eqs. (18) and (19), respectively:

$$C^{\text{U}} = \min\left\{\lambda C_{(s\to r,d)}\ ;\ \lambda C_{(s\to d)} + (1-\lambda)C_{(r\to d)}\right\}\ , \quad (18)$$

$$C^{\text{L}} = \min\left\{\lambda C_{(s\to r)}\ ;\ \lambda C_{(s\to d)} + (1-\lambda)C_{(r\to d)}\right\}\ , \quad (19)$$

where $C_{(a\to b,c)}$ is the capacity of the channel between the transmitter at node a and the receivers at both node b and node c. Similarly, $C_{(a\to b)}$ is the capacity of the channel between the transmitter at node a and the receiver at node b. Furthermore, $\lambda = N_s/(N_s + N_r)$ is the ratio of the first transmission period to the total transmission period. We have $\lambda = 0.5$ in the proposed scheme. The 16QAM-based upper and lower capacity bounds of the two-hop half-duplex relay network are portrayed in Fig. 7, which are computed based on the reduced-distance-related geometrical-gains of $G_{sr} = 6.83$ and $G_{rd} = 2.62$ as computed in Section IV.

The non-cooperative TTCM-VLC benchmark scheme has an effective throughput of $\eta_0 = N_i/N_s \approx 2.6$ bps, which is twice that of its cooperative counterpart. According to the 16QAM-based DCMC capacity curve of Fig. 7, the corresponding SNR_t (or SNR_r) at a throughput of $\eta_0 = 2.6$ bps is 10.03 dB. By contrast, the proposed DSCM and DSCM-O schemes have a throughput of $\eta = 1.3$ bps, while the corresponding SNR_t values for the upper and lower relay channel capacity bounds are 0.86 dB and 1.68 dB, respectively.

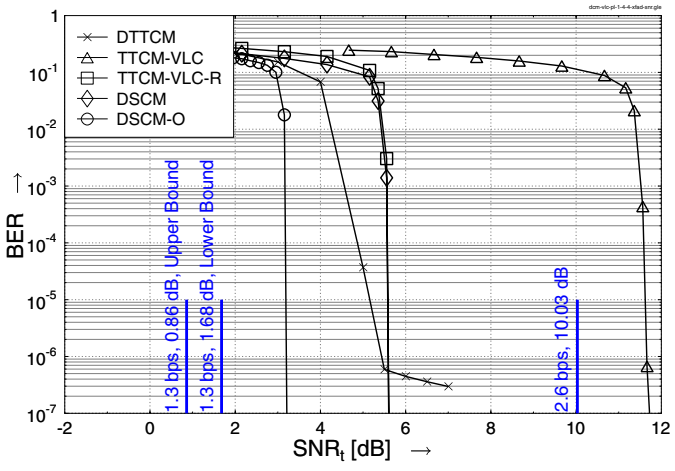

Fig. 8. BER versus SNR_t performance of the DTTCM [19], TTCM-VLC [11], TTCM-VLC-R, DSCM and DSCM-O schemes when communicating over uncorrelated Rayleigh fading channel using a frame length of $N_s = 15\,000$ symbols.

In order to benchmark our proposed schemes, we have considered the cooperative DTTCM scheme of [19], the non-cooperative TTCM-VLC scheme of [11] as well as a cooperative scheme referred to as TTCM-VLC-R, which does not consider the source-to-destination link, but employs a TTCM-VLC encoder at both the source and relay nodes. The BER versus SNR_t performance curves of the

DTTCM [19], TTCM-VLC [11], TTCM-VLC-R, DSCM and DSCM-O schemes communicating over uncorrelated Rayleigh fading channels using a frame length of $N_s = 15\ 000$ symbols are shown in Fig. 8. Since the minimum required receive SNR values at both the relay and destination nodes are the same for the TTCM-VLC-R arrangement, its optimal relay location is at the mid-point between the source and destination nodes. The BER performance of the TTCM-VLC-R scheme is almost identical to that of the DSCM scheme, which is $10\log_{10}(G_{rd}) = 6$ dB better than that of the non-cooperative TTCM-VLC scheme, since we have $G_{rd} = 4$ when the relay is located in the middle of the source-to-destination path. Note that if a path loss exponent of $\alpha = 4$ (e.g. suburban [21]) is used, we have $G_{rd} = 16$ when the relay is located in the middle of the source-to-destination path. Idealistic source encoder is assumed for the DTTCM scheme of [19] resulting in a throughput of 1.33 bps, which is close to that of the DSCM and DSCM-O schemes. Similar to the TTCM-VLC-R and DSCM arrangements, the DTTCM scheme employs a relay at the middle of the source-to-destination path. As seen in Fig. 8, the DTTCM scheme outperforms the TTCM-VLC-R and DSCM schemes in the SNR range before its BER floor starts to dominate its performance. By contrast, the TTCM-VLC-R and DSCM schemes do not suffer from a BER floor, because they benefit from iterative detection exchanging extrinsic information with a serially-concatenated outer VLC decoder.

As seen in Fig. 8, the proposed DSCM-O scheme employing a relay located at the optimum position managed to outperform all its counterparts. At a BER of 10^{-5}, the proposed DSCM-O scheme is $3.15 - 0.86 = 2.29$ dB and $3.15 - 1.68 = 1.47$ dB away from the corresponding upper and lower relay channel capacity bounds, respectively. We can further approach this relay channel capacity bound by minimising the area of the tunnel between the EXIT curves of the TTCM-VLC and TCM decoders shown in the EXIT chart of Fig. 6. This can be achieved by employing an irregular channel encoder instead of the TCM encoder at the relay node. However, this would impose a higher encoding and decoding complexity on the system. The DSCM-O scheme also outperforms the DTTCM and TTCM-VLC schemes by approximately 2 dB and 8.5 dB, respectively, at BER=10^{-5}. Furthermore, the BER of the DSCM-O scheme is lower than 10^{-7} at $\text{SNR}_t = 3.15$ dB, which is accurately predicted by its EXIT chart seen in Fig. 6.

VI. Conclusion

The serially concatenated TTCM-VLC of [11] is an attractive jointly optimised source-coding, channel-coding and modulation scheme. We have shown in this contribution that it is possible to save another 8.5 dB of transmit power, when the TTCM-VLC scheme is assisted by a simple TCM-aided relay node. The proposed DSCM-O scheme also outperforms the cooperative DTTCM scheme of [19] by approximately 2 dB and it is only about 1.47 dB away from the lower bound of the corresponding relay channel capacity. The proposed power and bandwidth efficient distributed source-coding, channel-coding and modulation scheme is capable of reducing the interference level in the mobile communication network due to the reduction of transmitting power. Hence, potentially more mobile users can be supported in rich mobile multimedia networks with the advent of the proposed scheme.

References

[1] P. Robertson and T. Wörz, "Bandwidth-efficient turbo trellis-coded modulation using punctured component codes," *IEEE Journal on Selected Areas in Communications*, vol. 16, pp. 206–218, Feb 1998.

[2] C. Berrou and A. Glavieux and P. Thitimajshima, "Near Shannon limit error-correcting coding and decoding: Turbo codes," in *Proceedings of the International Conference on Communications*, (Geneva, Switzerland), pp. 1064–1070, May 1993.

[3] S. Benedetto and G. Montorsi, "Design of parallel concatenated convolutional codes," *IEEE Transactions on Communications*, vol. 44, pp. 591–600, May 1996.

[4] G. Ungerböck, "Channel coding with multilevel/phase signals," *IEEE Transactions on Information Theory*, vol. IT-28, pp. 55–67, January 1982.

[5] S. X. Ng, O. Alamri, Y. Li, J. Kliewer and L. Hanzo, "Near-capacity turbo trellis coded modulation design based on EXIT charts and union bounds," *IEEE Transactions on Communications*, vol. 56, pp. 2030–2039, December 2008.

[6] S. ten Brink, "Convergence behaviour of iteratively decoded parallel concatenated codes," *IEEE Transactions on Communications*, vol. 49, pp. 1727–1737, October 2001.

[7] J. Kliewer, S. X. Ng, and L. Hanzo, "Efficient computation of EXIT functions for non-binary iterative decoding," *IEEE Transactions on Communications*, vol. 54, pp. 2133–2136, December 2006.

[8] R. Bauer, J. Hagenauer, "On variable length codes for iterative source/channel decoding," in *IEEE Data Compression Conference*, (UT, USA), pp. 273–282, 27-29 March 2001.

[9] V. B. Balakirsky, "Joint source-channel coding with variable length codes," in *IEEE International Symposium on Information Theory*, (Ulm, Germany), p. 419, 29 June – 4 July 1997.

[10] Y. Takishima, M. Wada and H. Murakami, "Reversible variable length codes," *IEEE Transactions on Communications*, vol. COM-43, no. 2/3/4, pp. 158–162, 1995.

[11] S. X. Ng, F. Guo, J. Wang, L-L. Yang and L. Hanzo, "Jointly optimised iterative source-coding, channel-coding and modulation for transmission over wireless channels," in *IEEE Vehicular Technology Conference Spring*, (Milan, Italy), pp. 313–317, 17-19 May 2004.

[12] V. Tarokh, N. Seshadri, and A. R. Calderbank, "Space-time codes for high data rate wireless communication: Performance criterion and code construction," *IEEE Transactions on Information Theory*, vol. 44, pp. 744–765, March 1998.

[13] G. Foschini Jr. and M. Gans, "On limits of wireless communication in a fading environment when using multiple antennas," *Wireless Personal Communications*, vol. 6, pp. 311–335, March 1998.

[14] E. Telatar, "Capacity of multi-antenna Gaussian channels," *European Transactions on Telecommunication*, vol. 10, pp. 585–595, Nov–Dec 1999.

[15] A. Sendonaris, E. Erkip and B. Aazhang, "User cooperation diversity part I: System description," *IEEE Transactions on Communications*, vol. 51(11), pp. 1927–1938, 2003.

[16] N. Laneman, D. N. C. Tse and G. W. Wornell, "Cooperative diversity in wireless networks: efficient protocols and outage behavior," *IEEE Trans. on Information Theory*, vol. 50, no. 12, pp. 3062–3080, 2004.

[17] E. Zimmermann, P. Herhold and G. Fettweis, "On the performance of cooperative relaying protocols in wireless networks," *European Transactions on Telecommunications*, vol. 16, no. 1, pp. 5–16, 2005.

[18] B. Zhao and M. C. Valenti, "Distributed turbo coded diversity for relay channel," *IEE Electronics Letters*, vol. 39, pp. 786–787, May 2003.

[19] S. X. Ng, Y. Li and L. Hanzo, "Distributed turbo trellis coded modulation for cooperative communications," in *Proceedings of International Conference on Communications (ICC)*, (Dresden, Germany), pp. 1–5, 14-18 June 2009.

[20] H, Ochiai, P. Mitran and V. Tarokh, "Design and analysis of collaborative diversity protocols for wireless sensor networks," in *Proceedings of IEEE VTC Fall*, (Los Angeles, USA), pp. 4645 – 4649, 26-29 September 2004.

[21] V. Erceg, L. J. Greenstein, S. Y. Tjandra, S. R. Parkoff, A. Gupta, B. Kulic, A. A. Julius and R. Bianchi, "An empirically based path loss model for wireless channels in suburban environments," *IEEE Journal on Selected Areas in Communications*, vol. 17, pp. 1205–1211, July 1999.

[22] R. G. Maunder, J. Wang, S. X. Ng and L. Hanzo, "On the performance and complexity of irregular variable length codes for near-capacity joint source and channel coding," *IEEE Transactions on Wireless Communications*, vol. 7, pp. 1338–1347, April 2008.

[23] J. G. Proakis, *Digital Communications*. New York: Mc-Graw Hill International Editions, 3rd ed., 1995.

[24] T. M. Cover and A. E. Gamal, "Capacity theorems for the relay channel," *IEEE Transactions on Information Theory*, vol. 25, pp. 572–584, Sept. 1979.

[25] A. Host-Madsen and J. Zhang, "Capacity bounds and power allocation for wireless relay channel," *IEEE Transactions on Information Theory*, vol. 51, pp. 2020–2040, Jun. 2005.